CEAS Aeronautical Journal (2026) 17:521–531
https://doi.org/10.1007/s13272-025-00864-9

ORIGINAL PAPER

Influence of vertical rotor spacing on aerodynamic efficiency of quadcopter configurations

Anna A. Kostek[1] · Johannes N. Braukmann[1] · Felix Lößle[1] · Antonio Visingardi[2] · Ronan Boisard[3] · Anthony D. Gardner[1]

Received: 4 December 2024 / Revised: 1 June 2025 / Accepted: 4 June 2025 / Published online: 26 June 2025

Abstract

The aerodynamic interactions in a quadcopter during forward flight reduce the efficiency of the back rotor(s) and increase generated noise levels. To alleviate interactions without compromising the vehicle's compactness, a vertical offset between the front and back rotor(s) can be introduced as an alternative solution to increased hub spacing. The efficiency of a quadcopter in square and diamond configuration with a vertical spacing up to 0.38 rotor diameter is analysed experimentally and numerically using free-wake solvers. Forward flight conditions are considered, including high interaction cases with a nose-up tilt and close rotor hub spacing with overlapping blades. The results show that for the square configuration, a thrust comparable to four isolated rotors is achieved by the elevation of both back rotors. In contrast, introducing a vertical separation to the already underperforming back rotor in the diamond configuration further reduces its efficiency.

Keywords Quadcopter · Vertical spacing · Panel method · Free wake · Interactions

Nomenclature

d	Horizontal rotor spacing [m]
D	Rotor diameter [m]
$\overline{P}$	Time-averaged power [W]
$\overline{Q}$	Time-averaged torque [Nm]
$\mathrm{d}T/\mathrm{d}r$	Sectional thrust [N/m]
$\mathrm{d}T_{single}/\mathrm{d}r$	Sectional thrust of an isolated rotor [N/m]
$\overline{T}$	Time-averaged thrust [N]
$\overline{T}_{single}$	Time-averaged thrust of an isolated rotor [N]
v_z	Out-of-plane velocity component [m/s]
V_∞	Flight velocity [m/s]
x_p	Coordinate of the rotor plane perpendicular to $\vec{V}_\infty$ [m]
y_p	Coordinate of the rotor plane in the downstream direction [m]
z	Vertical rotor spacing [m]
α_R	Tilt angle [°]
μ	Advance ratio [-]
σ	Solidity [-]
ω	Angular velocity [rad/s]

†These authors contributed equally to this work.

✉ Anna A. Kostek
anna.kostek@dlr.de

Johannes N. Braukmann
johannes.braukmann@dlr.de

Felix Lößle
felix.loessle@dlr.de

Antonio Visingardi
a.visingardi@cira.it

Ronan Boisard
ronan.boisard@onera.fr

Anthony D. Gardner
tony.gardner@dlr.de

1 German Aerospace Center (DLR), Göttingen, Germany

2 Italian Aerospace Research Center (CIRA), Capua, Italy

3 French Aerospace Lab (ONERA), Meudon, France

1 Introduction

Over the past decade, multicopters have dominated the unmanned aerial vehicles (UAV) market, with applications in diverse fields such as surveillance, videography, and remote site inspection [17]. Nevertheless, dedicated research has not kept pace with the ever-increasing popularity of multicopters and their limitations, including low endurance and high noise emission, remain unresolved. The sources of these problems can be found in the aerodynamic rotor interactions, which represent a complex phenomenon determined by flight conditions (advance ratio, tilt angle, etc.) and design parameters such as rotor spacing [4, 7, 13].

The interactions play a significant role during the forward flight when the wakes propagating closer to the rotor plane cause changes in the inflow conditions on adjacent rotors and increase the probability of blade vortex interactions (BVI) [9]. Strong adverse effects are observed for the back rotors affected by the downwash from the preceding rotors [3, 7, 18]. At the same time, although to a lesser extent, the vicinity of the rotors in the downstream region improves the efficiency of the front rotors [2, 11]. Additionally, the upwash on the outer wake edges caused by rolled up tip vortices can also improve the rotor efficiency for rotors located sideways or diagonally [14]. For the fixed-pitch rotors, typically used in multicopters, the interactions in forward flight are influenced by the wake asymmetry with a strong advancing side vortex propagating steeper downwards and a weaker retreating side vortex remaining closer to the blades.

A negative impact of the downwash on the back rotor(s) can be reduced by increasing the horizontal rotor spacing, as shown in the measurements of Atte et al. [3]. Studies by Healy et al. [7, 8] and Lee at al. [13] demonstrated that the introduction of a vertical offset is more effective for mitigating the adverse interaction effects without extending the vehicle size. The advantage of a vertical offset was also identified in the numerical study of the SUI Endurance quadcopter by Diaz and Yoon [19], which showed a 63% thrust increase achieved by undermounting the front rotors. Nevertheless, the measurements of a tandem configuration by Cai et al. [6] indicated the limitations of this approach with no further benefits on the rear rotor reached for the spacing higher than $d/D = 0.5$. In the following experimental study of a quadrotor by Atte et al. [2] up to 24% thrust increase was achieved with the vertical offset for the square (cross/'x') configuration, while the effect on the back rotor in the diamond (plus/'+') configuration depended on its horizontal distance from the side rotors.

Despite the existing research, the question of how to maximise the benefits of introducing vertical rotor separation remains unresolved due to a limited understanding of the resulting changes in rotor-rotor interactions. The objective of this study is to enhance existing knowledge on this topic by combining the experimental data with mid-fidelity free wake computations of a quadcopter in forward flight. The preceding investigation [11] showed a reduced efficiency of the square configuration for horizontal rotor spacings up to $d/D = 1.68$, with increasingly adverse effects observed for nose-up tilt angles. The improved efficiency of the front rotors due to tandem and side-by-side arrangement interactions was not sufficient to compensate for the efficiency loss on the back rotors. In contrast, the diamond configuration showed improved efficiency for all hub spacings with no overlapping rotors. The rearmost rotor was the only rotor affected by negative interaction effects. The present study aims to verify whether adding a vertical offset to the back rotors in the square configuration or to the rearmost rotor in a diamond configuration can effectively improve, or respectively further improve, the quadrotor efficiency.

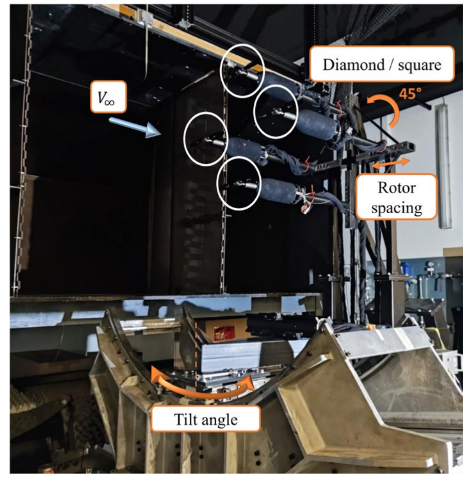

Fig. 1 Experimental setup with investigated parameters [11]

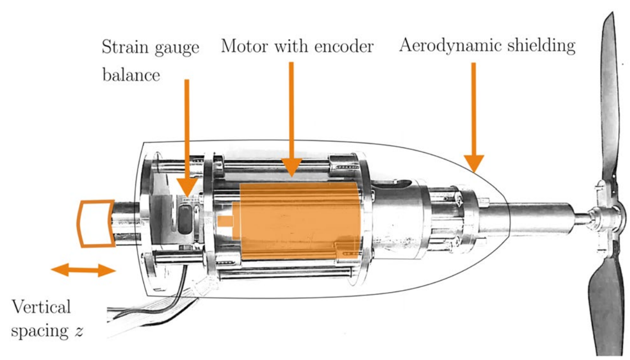

Fig. 2 Setup of the drive unit [10]

2 Experimental setup

The quadrotor experiment was conducted in the RTG (rotor test facility Göttingen) wind tunnel at the German Aerospace Center (DLR) with the setup presented in Fig. 1. Fixed-pitch, two-bladed KDE 12.5x4.3" rotors with a diameter of 0.318m and solidity of $\sigma = 0.075$ were used. The rotors were driven by 180 W Maxon EC-i 52 brushless motors with ENC 16 EASY encoders (Fig. 2). Custom blade adapters were used to facilitate the mounting of the rotors on the shafts and to eliminate lead-lag movement. The rotors were operated with a constant rotational speed of 5400 RPM at a wind velocity $V_\infty = 12.9$ m/s, which corresponds to the advance ratio $\mu = 0.146$.

The thrust of each rotor was measured using a one-axis strain gauge sensors KD40s from ME Messsysteme and the torque was evaluated based on the electric power consumption [10]. Different rotor arrangements relative to the flight direction were investigated with a rotor frame changed between the square and diamond configuration (Fig.3). In contrast to the previous study [11], only one rotation direction of the rotors was considered for the square configuration as the influence of changing the rotor direction was secondary to the change in rotor arrangement. The square bearhug configuration was selected, with the front rotors rotating inwards and the back rotors rotating outwards. For the diamond configuration, a counterclockwise rotation direction of the front and the back rotor as well as a clockwise rotation of both side rotors was used.

The rotor frame was mounted on a rotatable base to allow for a variation of the rotor plane tilt angle α_R typical for the forward flight conditions. The study was focused on cases with $-10°$ tilt (nose-down) and $10°$ (nose-up). The two angles represent characteristic forward flight modes ensuring the forward propulsion and braking, respectively. As shown in Fig.4, the nose-up tilt results in stronger self and mutually induced aerodynamic interactions with the back rotors operating directly in the wake of the front rotors as well as ingesting their own wakes.

The influence of varying the vertical distance between the rotors was investigated for the horizontal (hub) spacings $d/D = 1.2$ and $d/D = 0.96$. The operation with overlapping rotor blades for the latter could be achieved by keeping a constant orthogonal rotor phasing. Both the back rotors in the square configuration and the aftmost rotor in the diamond configuration were raised above the front rotors' plane. For this purpose, a vertical offset z in the steps of 0.12 D, 0.26 D, 0.38 D was applied using metal distance rings of corresponding heights at the rotor mounting shown in Fig. 2. The maximum vertical offset $z/D = 0.38$ at the horizontal spacing $d/D = 1.2$ was not analysed for the square configuration due to interference between the elevated aerodynamic shieldings and the front rotors' wakes.

3 Computational tools

The measurements were compared with computational results from free-wake solvers, including blade models with finite thickness (UPM and RAMSYS) and a lifting-line model corrected with viscous airfoil characteristics (PUMA). The main focus of the study remains the effect of rotor height offset, with UPM results serving as the primary reference for the discussion. Results from the additional solvers are included to validate the robustness of the observed trends, accounting for solver-dependent differences in modeling and the treatment of viscous effects, shown to introduce potential errors [11].

3.1 UPM

Unsteady panel method (UPM) is a free wake tool developed at DLR, which allows simulations of potential flows with arbitrary body shapes and motion [1, 21]. The distribution of sources and sinks on the blade surface simulate the blade thickness, while the lift is modelled by the prescribed

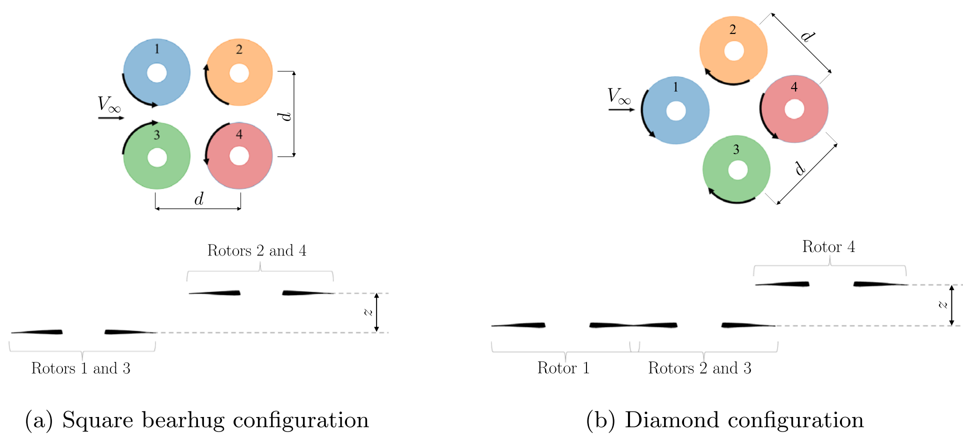

Fig. 3 Definition of the horizontal spacing d and vertical spacing z between the rotors

Fig. 4 Wakes represented as a vortex lattice at analysed tilt angles α_R [12]

weighting function of vortices on the chord surface panels. The Kutta condition is satisfied through a zero-thickness elongation of the trailing edge by ensuring pressure equality on the lower and upper surface. The blade model with a root cutout of 0.3 rotor radii and a sharp trailing edge was prepared with a panel generation code PANGEN based on a 3D scanned geometry [12]. The simulations were performed for up to 9 rotor revolutions with an initial step size of 5° reduced to 2° during the computation.

3.2 RAMSYS

CIRA (Italian Aerospace Research Center) applied the in house-developed mid-fidelity computer code RAMSYS (Rotorcraft Aerodynamic Modelling SYStem), specifically created for the aerodynamic analysis of multirotor and multibody configurations [20]. The solver is based on the boundary element methodology (BEM) for the solution of inviscid, unsteady, incompressible flows and applies Morino's boundary integral formulation to Laplace equation [15] for the evaluation of the velocity potential. The surface pressure distribution on the configuration is calculated using the velocity potential by means of the unsteady Bernoulli equation, which is then integrated to evaluate the forces and moments acting on the configuration. A computational acceleration is obtained by applying the parallel execution via the OpenMP API. Calculations were made with an azimuth step of 2° and considering six rotor revolutions with six wake spirals.

3.3 PUMA

ONERA (French Aerospace Lab) computations were performed using the in-house mid-fidelity solver PUMA. It is based on the lifting line theory coupled with the free wake panel method [16] and benefit from the Fast Multipole Method implementation to speed up the process of induced velocity computations. This tool has already shown its ability to simulate rotor – rotor interactions in a various range of configurations such as those studied by Boisard et al. [5] and Kostek et al. [11]. In the current study, the lifting line was divided into 45 sections in a square root distribution and the 2D airfoil data used for the lifting line evaluation were provided by DLR. The time step was set to 5° azimuth and computation was performed over at least 8 revolutions.

4 Results

The influence of the vertical offset is evaluated based on the difference in loads relative to the single rotor results (Table 1). The mean values of thrust ($\overline{T}$) and torque ($\overline{Q}$) from the computations were time-averaged over one rotor revolution. The efficiency in forward flight was evaluated from the power loading defined as $\frac{\overline{T}}{\overline{P}} = \frac{\overline{T}}{\overline{Q}\omega}$. While the measured torque remained nearly constant for the analysed cases (maximum variations of 2%), changes in the efficiency were reflected in the changes of thrust, which therefore represent a key focus of the study.

Table 1 Mean thrust and torque of a single rotor ($\bar{T}_{\text{single}}$, $\bar{Q}_{\text{single}}$), 5400 RPM, $V_\infty = 12.9$ m/s

		Experiment	UPM	RAMSYS	PUMA
$\bar{T}_{\text{single}}$[N]	−10°	7.37	7.13	7.048	7.13
	+10°	10.19	10.08	9.73	9.91
$\bar{Q}_{\text{single}}$[Nm]	−10°	0.09	0.081*	0.083*	0.099
*inviscid	+10°	0.064	0.057*	0.061*	0.082

Figures 5, 6 show the mean thrust $\overline{T}$ of two quadrotor configurations, compared with that of four isolated rotors for vertical spacings up to *z/D* = 0.38. As shown by all results in Fig. 5, elevating the back rotors in the square configuration immediately improves the quadrotor efficiency at a tilt angle of −10°. For both hub spacings, a gradual increase in thrust is obtained with an increasing vertical offset. At a hub spacing of *d/D* = 0.96 a vertical offset of *z/D* = 0.15 is sufficient to eliminate the detrimental downwash influence. Further increases in the vertical spacing at the nose-down tilt result in an increase in produced thrust (below 5%) compared to four isolated rotors. Nevertheless, the trend indicates that adding an offset greater than *z/D* = 0.38 would not result in a significant further increase in thrust. The same is true of the hub spacing *d/D* = 1.2, for which no thrust gain over four isolated rotors is achieved. In contrast to the immediate benefits observed at the −10° tilt angle, the increase in efficiency for the smallest vertical spacing at the nose-up angle of 10° is negligible. In the case of *d/D* = 1.2, no more than a 1% efficiency improvement is observed below *z/D* = 0.12. However, for both vertical spacings, up to 10% efficiency improvement is achieved by rising the back rotors by *z/D* = 0.38. Consequently, according to the measurement, the configuration with the horizontal spacing of *d/D* = 0.96 reaches the efficiency of four isolated rotors. As shown in the computational results, the maximum efficiency for the *d/D* = 1.2 case is at least 5% lower.

In contrast, elevating the back rotor in the diamond configuration does not improve the aerodynamic efficiency (Fig. 6). According to the measurement, the benefit from the interactions visible at *z/D* = 0 is reduced by up to 4% for both horizontal spacings. The quadrotor efficiency remains nearly constant with an increase in the vertical offset above *z/D* = 0.26.

The described effects are studied in detail in the following subsections based on the efficiency analysis of individual rotors. The complex rotor interactions in the quadrotor

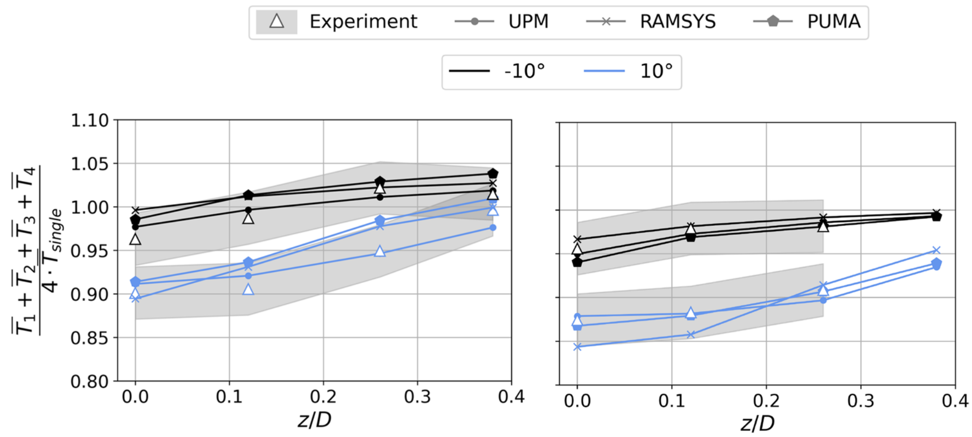

(a) d/D=0.96 (b) d/D=1.2

Fig. 5 Change in mean thrust of the square bearhug configuration with varying vertical rotor offset

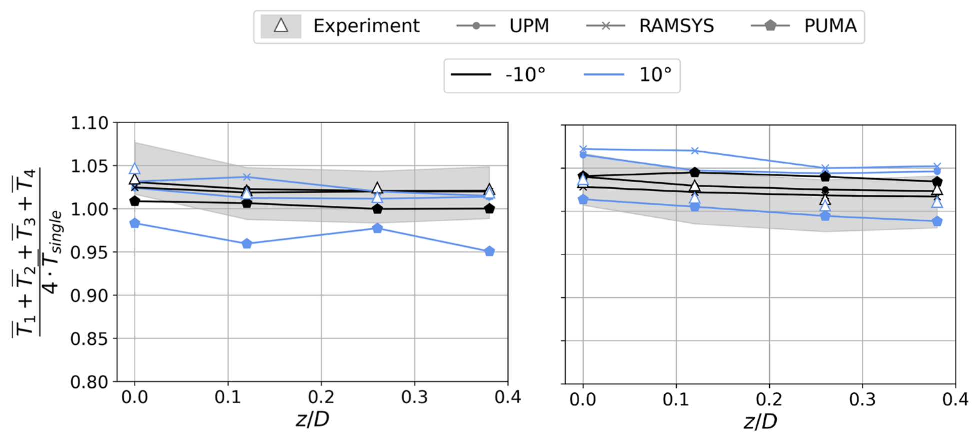

(a) d/D=0.96 (b) d/D=1.2

Fig. 6 Change in mean thrust of the diamond configuration with varying vertical rotor offset

configurations (Fig. 7a, b) are easier to understand based on the wake of the isolated rotor, visualised in Fig. 7c . A clear asymmetry of the wake can be observed between the rolled-up tip vortices with an advancing side vortex propagating steeply downwards and a retreating side vortex staying closer to the rotor plane.

4.1 Square configuration

Figure 8 shows the change in thrust compared to an isolated rotor for rotors 3 and 4, representing both the front and both the back rotors respectively. As shown by computational and experimental results, the introduction of a vertical offset to the back rotors improves their efficiency in all cases analysed. The thrust produced by each back rotor is increased by approximately 10% at −10° tilt angle and 20% at 10°, which, according to the measurements, is still not sufficient to reach the isolated rotor's efficiency. Nevertheless, even though full recovery is not achieved for rotors 2 and 4, the increased thrust of the front rotors improves the overall quadrotor efficiency. As shown in Fig. 9, a positive impact of the tandem interaction on the front rotor, visible around 0° azimuth, weakens as the vertical spacing between the front and back rotors increases. At the same time, a strong side-by-side interaction with a neighbouring rotor at 270° azimuth remains nearly unchanged, resulting in an approximately constant 10% thrust increase for rotors 1 and 3 at $z/D = 0.96$. The interactions between the front rotors at the wider hub spacing $d/D = 1.2$ are not as strong, yet the benefit is clearly observable for all z/D values.

At $z/D = 0$ the thrust loss on the back rotors is comparable for both horizontal spacings. However, an introduction of the vertical offset gives better results for the configuration with the blade overlap ($d/D = 0.96$). Figure 10 shows that non-elevated back rotors are affected by the downwash from the advancing side vortex of the preceding rotor for both cases. Raising the back rotors reduces the interaction on this side; however, the rotors are then more influenced by the retreating side vortex propagating at increased z-position (as shown in Fig. 7). This interaction persists at larger vertical

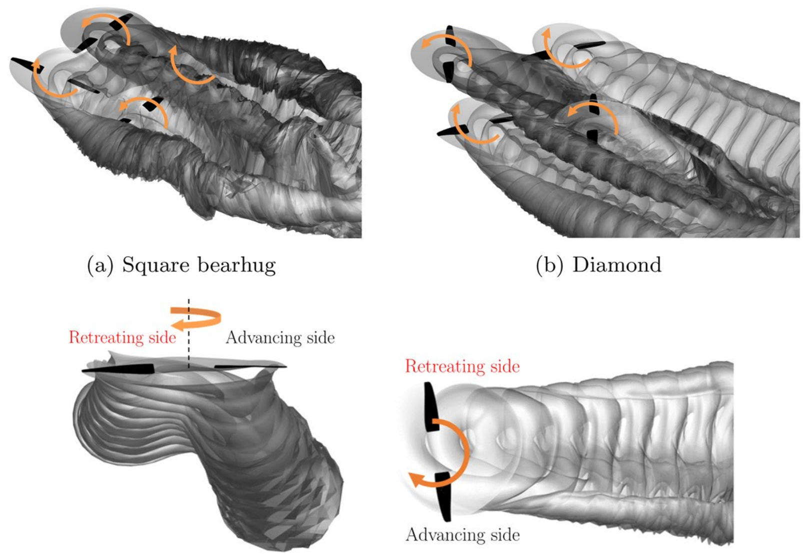

(a) Square bearhug (b) Diamond

(c) Isolated rotor (front and top view)

Fig. 7 Rotor wakes visualized in UPM with a vortex lattice

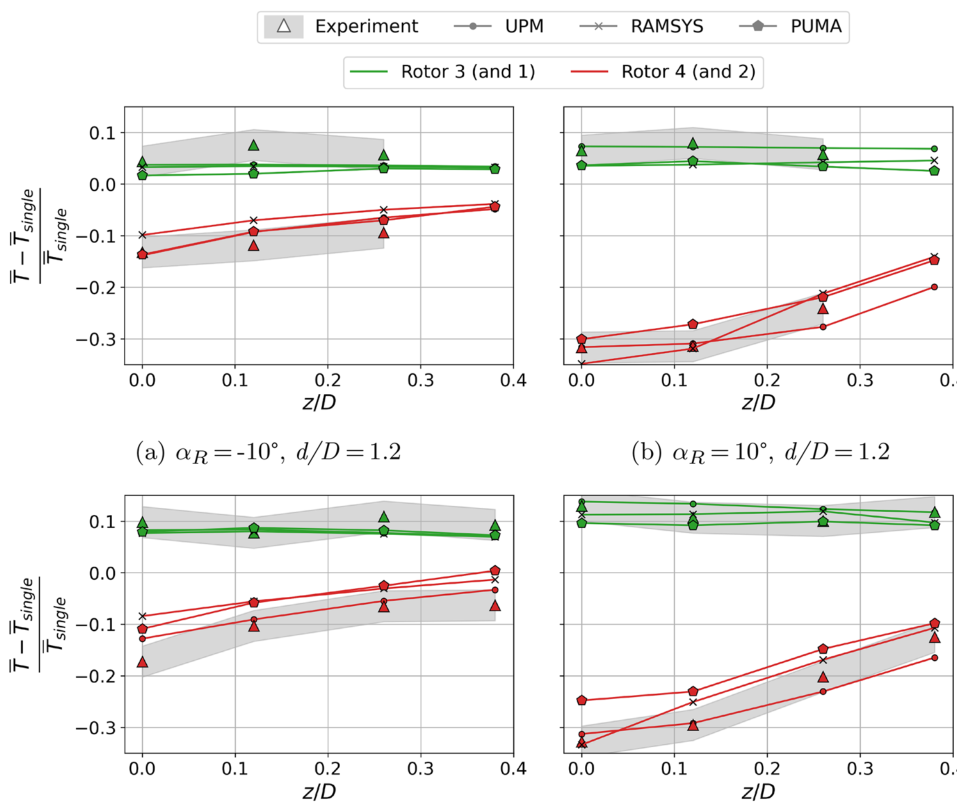

(a) $\alpha_R = \text{-}10°,\ d/D = 1.2$ (b) $\alpha_R = 10°,\ d/D = 1.2$

(c) $\alpha_R = \text{-}10°,\ d/D = 0.96$ (d) $\alpha_R = 10°,\ d/D = 0.96$

Fig. 8 Change in mean thrust of each rotor in square bearhug configuration with varying vertical rotor offset

spacings for $d/D = 1.2$, for which the trajectory of the vortices is no longer aligned with the back rotors.

Regardless of the horizontal separation in the square configuration at 10° tilt angle, the impact of the retreating side tip vortices on the back rotors is observable even for the largest vertical offset. This is surprising when considering the wake trajectory of an isolated rotor (Fig. 11a). As shown, the retreating side tip vortex of the upstream rotor propagates in the rotor plane, well below the theoretical position of the downstream rotor. However, as presented in

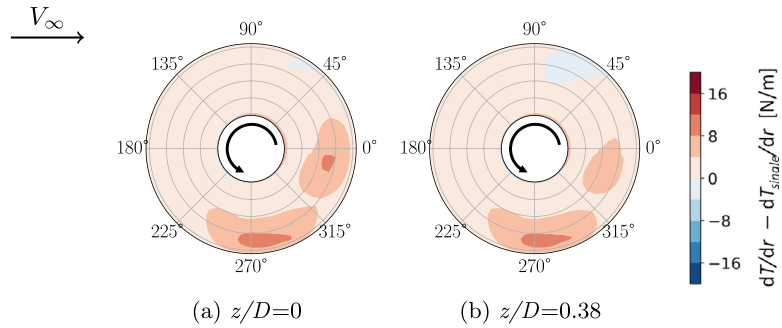

(a) z/D=0 (b) z/D=0.38

Fig. 9 Change in thrust of rotor 1 in the square bearhug configuration with tilt −10° and *d/D*= 0.96 (UPM)

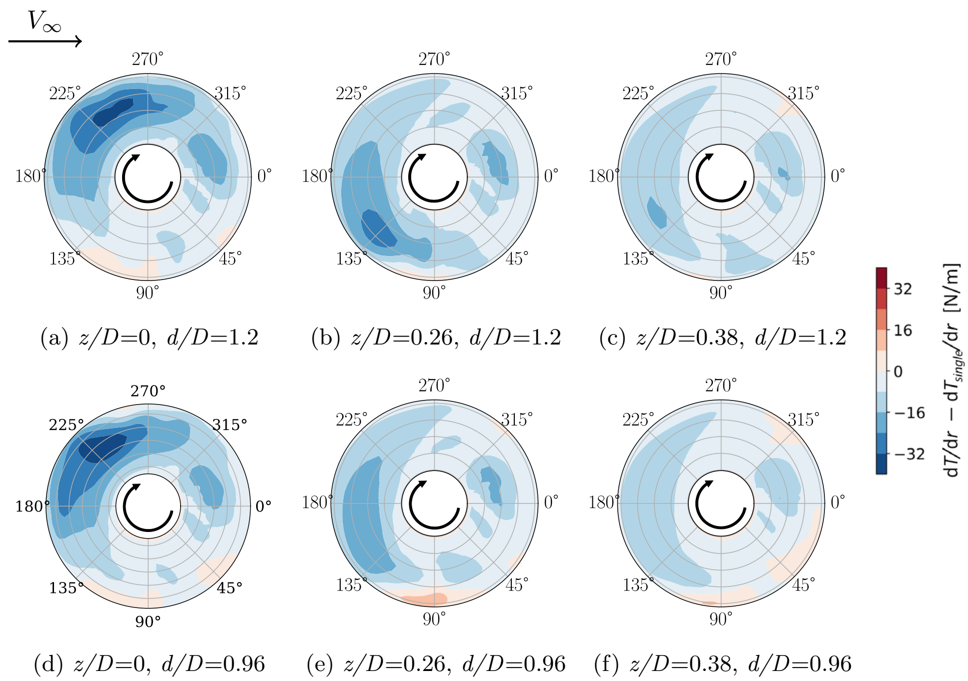

Fig. 10 Change in thrust of rotor 2 in the square bearhug configuration with tilt 10° (UPM)

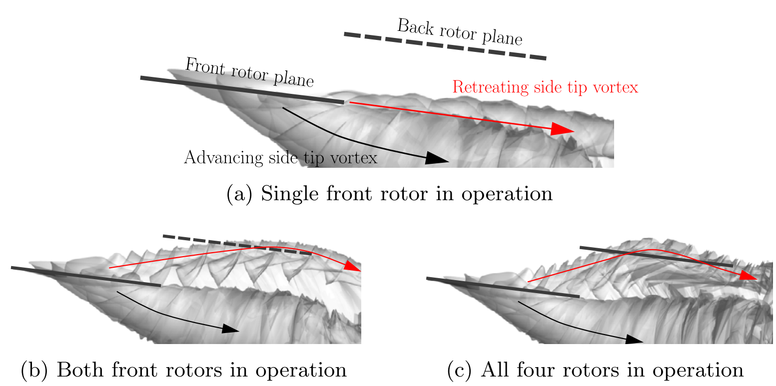

Fig. 11 Wake of the front rotor(s) in square bearhug configuration at 10° tilt angle, *d/D*=0.96 and *z/D*=0.38; represented as a vortex lattice

Fig. 11b , a bearhug interaction between the front rotors changes the trajectory of their inboard tip vortices, directing them upwards. In a full configuration an upwash region is also generated between the back rotors, which further deflects the vortex trajectory towards the back rotor. As a result, detrimental downwash influence is observable in this region for larger vertical offsets than expected from the wake geometry of the single rotor.

4.2 Diamond configuration

Elevation of the back rotor in the diamond configuration does not have a significant influence on the efficiency of the preceding rotors. For this reason, Fig. 12 focuses on the results for rotor 4 with experimental data for rotors 1, 2 and 3 added as a reference.

According to the measurements, adding the vertical offset to the back rotor reduces its thrust by up to 10% at $d/D = 1.2$. All results show that at 10° tilt angle the thrust reduction is already observed for $z/D = 0.12$ and it remains almost constant with further increasing z spacing. For $d/D = 0.96$ the back rotor shows the lowest efficiency at $z/D = 0.12$. Its thrust increases with greater vertical offsets, yet no improvement compared to the efficiency at $z/D = 0$ is achieved. The explanation for the observed tendency can be found in the changes of sectional thrust dT/dr compared to an isolated rotor (Fig. 13).

Unlike the square configuration, the back rotor in the diamond system is affected not only by the detrimental tandem interaction with the front rotor but also by diagonal alignment interactions with the side rotors. However, these can have either positive or negative influence on rotor efficiency depending on the flight conditions and distances between the rotors. For a larger horizontal spacing $d/D = 1.2$ at the tilt angle of $-10°$, the vortex from the advancing side of rotor 2 causes a local thrust reduction on rotor 4 (Fig. 13a). This adverse effect is almost entirely cancelled out by the upwash created by the rolled-up retreating side vortex of rotor 3. Adding a vertical offset to the back rotor gradually reduces the downwash impact on the advancing side, but also completely eliminates the positive upwash influence (Fig. 13b, c). As the detrimental effect of the advancing side vortex remains observable for all vertical spacings, the rotor thrust is reduced compared to the $z/D = 0$ case. Additionally, a progressive thrust decrease at the front of rotor 4 indicates more interaction with the wake of rotor 1 for larger z spacings. Similarly, at $d/D = 0.96$ and no vertical offset, the back rotor is mainly influenced by the side rotors' tip vortices, both of which in this case cause strong local downwash regions (Fig. 13d). At the same time, an upwash area between the side rotors counteracts the downwash from rotor 1 around 180° azimuth of rotor 4 (Fig. 14a). After raising the back rotor by $z/D = 0.12$ the influence of the side rotors slowly decreases, yet the back rotor also loses its shielding from the tandem interaction (Fig. 14b). As a result, the thrust loss area spreads to the entire front of the rotor 4 (Fig. 13e). The thrust gradually improves with further increases in the vertical spacing (Fig. 13f); however, no improvement

Fig. 12 Change in mean thrust of each rotor in the diamond configuration with varying vertical rotor offset

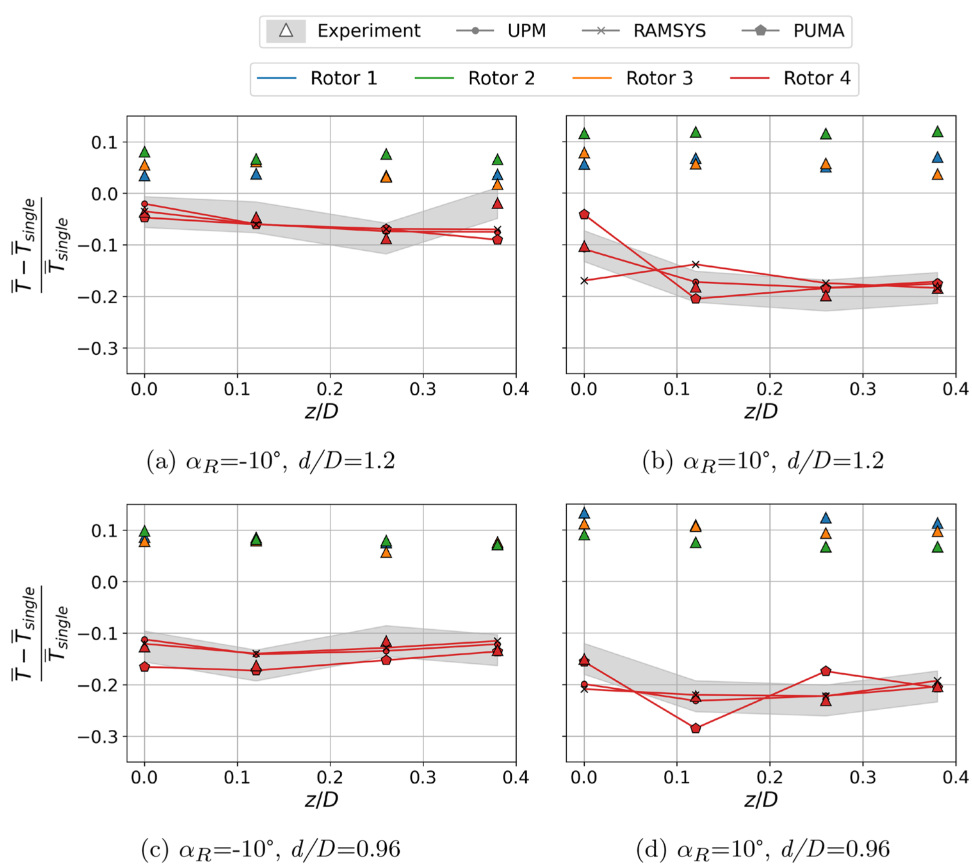

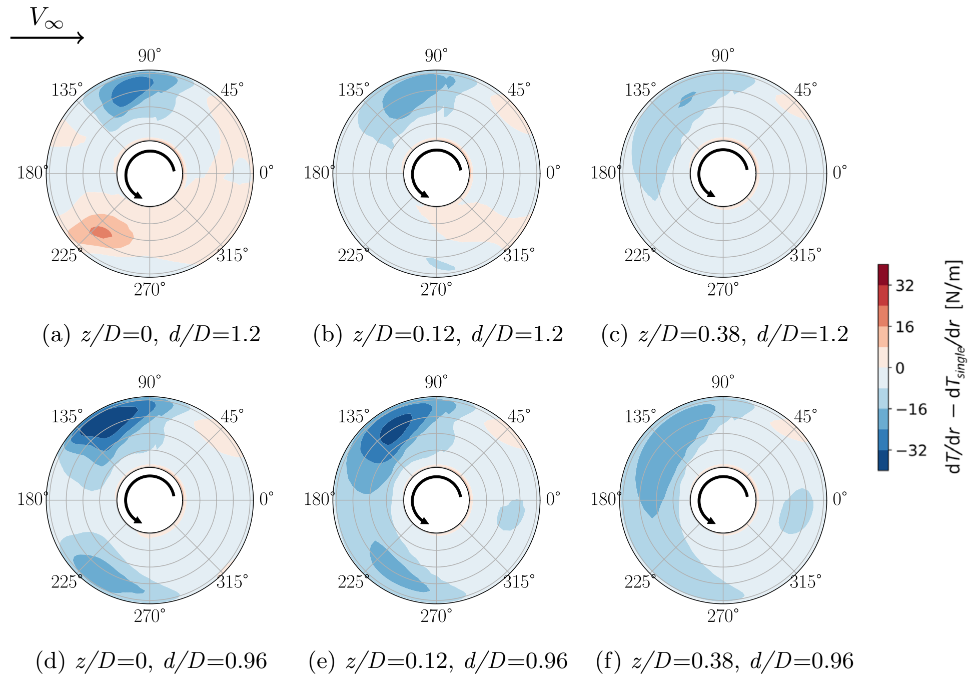

Fig. 13 Change in thrust of rotor 4 in the diamond configuration with tilt −10° (UPM)

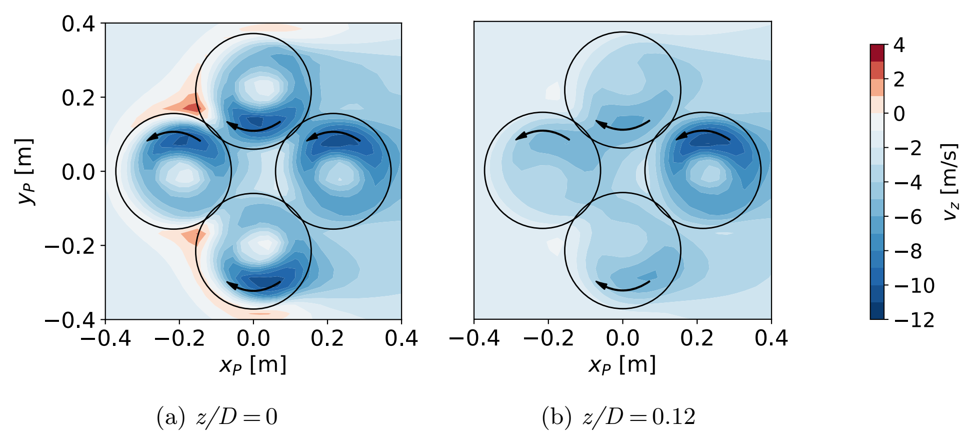

Fig. 14 Velocity field in the plane of rotor 4, $\alpha_R = -10°$ and $d/D = 0.96$ (UPM)

compared to $z/D = 0$ is achieved within the vertical offsets which are analysed.

5 Discussion

The results show that elevating the back rotors is a more efficient method of improving the square quadcopter efficiency than increasing the horizontal hub spacing. This is particularly evident for the 10° tilt angle, where increasing the hub separation did not enhance the back rotors' efficiency and only cancelled a positive proximity effect for the front rotors within the analysed d values [11]. Nevertheless, the benefit of introducing a vertical offset strongly depends on the quadrotor tilt angle and effectively means that the strongest interactions with a preceding rotor wake are shifted to higher

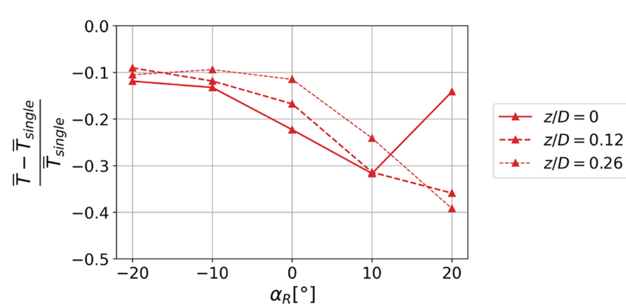

Fig. 15 Change of thrust of the back rotor in the square bearhug configuration depending on the tilt angle and vertical offset, d/D=1.2

nose-up tilt angles. Figure 15 shows that at $z/D = 0$ the back rotor recovers from the downwash influence above $\alpha_R = 10°$. From this point on, a vertical offset has a detrimental effect as it causes a further thrust reduction. The resulting loss on the raised rotors at $\alpha_R = 20°$ is greater than the maximum loss with $z/D = 0$ at $\alpha_R = 10°$.

Prediction of the front rotors' wake trajectory, including asymmetric wake propagation, is necessary to assess the vertical offset benefit. The trajectory of the retreating side vortices is determined by the wake-wake interaction from the bearhug alignment between the front rotors. The influence of the front rotors' wake trajectory is expected to be less significant for the square breaststroke configuration (the front rotors rotating outwards) with the advancing side vortices interacting.

The qualitative efficiency changes caused by the vertical offset were captured by all mid-fidelity tools applied. The largest discrepancies up to 6% are observed in the thrust prediction of the diamond configuration at the nose-up tilt angle. The differences in this case mostly come from strong upwash interactions on rotor 2 causing flow separation, which is not accounted for in the inviscid results of UPM and RAMSYS as described by Kostek et al. [11].

6 Conclusions

Introducing a vertical offset to the back rotors in the square configuration improves its thrust up to 5% at −10° tilt angle and 11% at 10° tilt. An efficiency comparable to or higher than four isolated rotors is achieved for the close horizontal rotor spacing $d/D = 0.96$. The side-by-side alignment interactions between the front rotors delay the vertical offset benefit so that at nose-up tilt angle the elevation higher than $z/D = 0.38$ is necessary to achieve a full recovery of the thrust of the back rotors.

In contrast, adding a vertical separation to the back rotor in the diamond configuration has a negative impact on its efficiency. At $z/D = 0$ inflow conditions around 180° azimuth of the back rotor are comparable to an isolated rotor case due to the upwash between the side rotors. The elevated back rotor is more exposed to the downwash from the wake of the frontmost rotor. A gradual improvement in the rotor efficiency is expected for vertical separation greater than $z/D = 0.38$ due to reduced downwash from all the preceding rotors.

The highest efficiency with up to 5% thrust increase compared with four isolated rotors is achieved for the square configuration with $d/D = 0.96$ and the vertical offset of $z/D = 0.38$ as well as for the diamond configuration with $d/D = 1.2$ and no vertical offset.

While the study focused on selected, typical flight conditions (e.g. advance ratio, tilt angles), the design of a quadcopter with a vertical spacing requires consideration of a wide range of parameters. Nevertheless, the results serve as a starting point and offer an insight into the potential aerodynamic benefits of introducing a vertical rotor offset depending on the configuration.

Acknowledgements The study was funded by the German Aerospace Center (DLR) as a part of the Urban Rescue Project. Cooperation between research facilities was enabled within the group GARTEUR AG-25 "Rotor-rotor wakes interactions". A part of this work has been previously presented at the conference Research & Education in Aircraft Design 2024 in Warsaw, Poland and published within the PhD thesis [12].

Funding Open Access funding enabled and organized by Projekt DEAL.

Data availability The presented data are accessible upon request, by contacting the corresponding author.

Declarations

Conflict of interest The authors declare no conflict of interest.

References

1. Ahmed, S.R., Vidjaja, V.T.: Unsteady panel method calculation of pressure distribution on BO 105 model rotor blades. J. Am. Helicopter Soc. **43**(1), 47–56 (1998). https://doi.org/10.4050/JAHS.43.47
2. Atte, A., Rauleder, J.: Investigation of Rotor Vertical Offset Effects on Quadrotor Performance. In: *Vertical Flight Society 80th Annual Forum*. Montreal, Canada, (2024) https://doi.org/10.4050/F-0080-2024-1388
3. Atte, A., Rauleder, J., Wylie, D.: Experimental Investigation of Multi- Rotor Aerodynamic Interactions. In: *Vertical Flight Society 78th Annual Forum*. Fort Worth, Texas, USA, (2022) https://doi.org/10.4050/F-0078-2022-17467
4. Barcelos, D., Kolaei, A., Bramesfeld, G.: Aerodynamic interactions of quadrotor configurations. J. Aircraft **57**(6), 1074–1090 (2020). https://doi.org/10.2514/1.C035614
5. Boisard, R.: Numerical analysis of rotor/propeller aerodynamic interactions on a high-speed compound helicopter. J. Ame. Helicop. Soc. **67**, 1 (2022). https://doi.org/10.4050/JAHS.67.012005
6. Cai, J., Gunasekaran, S., Ol, M.: "Vertically Offset Overlapping Propellers in Tandem Configuration". In: *AIAA SciTech Forum*. National Harbor, MD & Online, (2023) https://doi.org/10.2514/6.2023-2464
7. Healy, R., Misiorowski, M., Gandhi, F.: A CFD-based examination of rotor-rotor separation effects on interactional aerodynamics for eVTOL aircraft. J. Am. Helicopter Soc. **67**(1), 1–12 (2022). https://doi.org/10.4050/JAHS.67.012006

8. Healy, R., Misiorowski, M., Gandhi, F.: A Systematic CFD-Based Examination of Rotor-Rotor Separation Effects on Interactional Aerodynamics for Large eVTOL Aircraft. In: *Vertical Flight Society 75th Annual Forum & Technology Display*. Virtual, (2019) https://doi.org/10.4050/F-0075-2019-14498
9. Hwang, J.Y., Jung, M.K., Kwon, O.J.: Numerical study of aerodynamic performance of a multirotor unmanned-aerial-vehicle configuration. J. Aircraft **52**(3), 839–846 (2015). https://doi.org/10.2514/1.C032828
10. Kostek, AA.: "Computational and Experimental Investigation of Quadrotor Aerodynamics and Aeroacoustics". PhD thesis. Germany: Leibniz University Hannover, (2024)
11. Kostek, A.A., Braukmann, J.N., Löle, F., Miesner, S., Visingardi, A., Boisard, R., Riziotis, V., Keler, M., Gardner, A.D.: Experimental and computational investigation of aerodynamic interactions in quadrotor configurations. J. Am. Helicopter Soc. **69**(2), 1–17 (2024). https://doi.org/10.4050/JAHS.69.022009
12. Kostek, A.A., Löle, F., Wickersheim, R., Keler, M., Boisard, R., Reboul, G., Visingardi, A., Barbarino, M., Gardner, A.D.: Experimental Investigation of UAV Rotor Aeroacoustics and Aerodynamics with Computational Cross-Validation. CEAS Aeronaut. J. (2023). https://doi.org/10.1007/s13272-023-00680-z
13. Lee, J., Oh, S., Yee, K., Kim, D.-K.: Numerical investigation on overlap effects of tandem rotors in forward flight. Int. J. Aeronaut. Space Sci. **10**(2), 63–76 (2009). https://doi.org/10.5139/IJASS.2009.10.2.063
14. Misiorowski, M., Gandhi, F., Oberai, A.A.: Computational study on rotor interactional effects for a quadcopter in edgewise flight. AIAA J. **57**(12), 5309–5319 (2019). https://doi.org/10.2514/1.J058369
15. Morino, L., Gennaretti, M., Petrocchi, P.: "A General Theory of Potential Aerodynamics with Applications to Helicopter Rotor-Fuselage Interaction". In: *Boundary Element Methods*. Berlin, Germany: Springer, (1992) 242–251 https://doi.org/10.1007/978-3-662-06153-4_27
16. Mudry, M.: "La Theorie Generale Des Nappes Et Filaments Tourbillonnaires Et Ses Applications a L'aerodynamique Instationnaire". PhD thesis. France: University of Paris, (1982)
17. Quan, Q.: *Introduction to Multicopter Design and Control*. Singapore: Springer, (2017) https://doi.org/10.1007/978-981-10-3382-7
18. Russell, C., Conley, S.: "The Multirotor Test Bed - A New NASA Test Capability for Advanced VTOL Rotorcraft Configurations". In: *Proceedings of the Vertical Flight Society 76th Annual Forum*. Vertical Flight Society 76th Annual Forum & Technology Display. Virtual, (2020) 1–12 https://doi.org/10.4050/F-0076-2020-16370
19. Ventura Diaz, P., Yoon, S.: High-Fidelity Computational Aerodynamics of Multi-Rotor Unmanned Aerial Vehicles. In: *AIAA SciTech Forum*. Kissimmee, Florida, (2018) https://doi.org/10.2514/6.2018-1266
20. Visingardi, A., D'Alascio, A., Pagano, A., Renzoni, P.: Validation of CIRA's Rotorcraft Aerodynamic Modelling System with DNW Experimental Data. In: *22nd European Rotorcraft Forum*. Brighton, UK, (1996)
21. Yin, J., Ahmed, S.R.: Helicopter main-rotor/tail-rotor interaction. J. Am. Helicopter Soc. **45**(4), 293–302 (2000). https://doi.org/10.4050/JAHS.45.293